Conformational change induced by electron transfer in a monolayer of cytochrome P450 reductase adsorbed at the Au(110)–phosphate buffer interface

P. Weightman,[1,*] C. I. Smith,[1] J. H. Convery,[1] P. Harrison,[1] B. Khara,[2] and N. S. Scrutton[2]

[1]*Department of Physics, Oliver Lodge Laboratory, University of Liverpool, Liverpool L69 7ZE, United Kingdom*

[2]*Faculty of Life Sciences, University of Manchester, Manchester Institute of Biotechnology, 131 Princess Street, Manchester M1 7DN, United Kingdom*

(Received 10 June 2013; published 26 September 2013)

The reflection anisotropy spectroscopy profiles of a variant of cytochrome P450 reductase adsorbed at the Au(110)–phosphate buffer interface depend on the sequence of potentials applied to the Au(110) electrode. It is suggested that this dependence arises from changes in the orientation of the isoalloxazine ring structures in the protein with respect to the Au(110) surface. This offers a method of monitoring conformational change in this protein by measuring variations in the reflection anisotropy spectrum arising from changes in the redox potential.

DOI: 10.1103/PhysRevE.88.032715 PACS number(s): 87.14.E−, 87.64.K−, 68.43.Mn

I. INTRODUCTION

Cytochrome P450 reductase (CPR) is an electron transfer flavoprotein that in living systems is anchored to a membrane [1] and that carries out its electron transfer function by large changes in the relative orientation of two structural parts of the protein: the flavin adenine dinucleotide (FAD)- and flavin mononucleotide (FMN)-binding domains [2,3]. Each domain supports an isoalloxazine ring structure that is able to vary its electron population from zero to two electrons (the oxidized, semiquinone, and dihydroquinone states). There are nine redox forms of CPR. Each is populated to a different extent in one- to four-electron-reduced CPR, based on the known redox potentials of the FAD and FMN flavin cofactors [4]. In previous work it was demonstrated that a variant of the protein can be assembled as an ordered monolayer on a Au(110)–phosphate buffer interface in both its oxidized [5] and reduced [6] forms mimicking the anchoring of the protein in the membrane. It has been shown previously that the technique of reflection anisotropy spectroscopy (RAS) can be used to monitor changes in the orientation of adenine adsorbed at a Au(110)–phosphate buffer interface as the potential applied to the Au(110) electrode is varied [7,8]. This opens up the possibility of using RAS to monitor conformational change on a millisecond timescale in cytochrome P450 reductase resulting from the transfer of electrons. This paper is part of a long term study directed at this aim [5,6,9] and describes the detailed changes that take place in the RAS of cytochrome P450 reductase adsorbed at Au(110)–phosphate buffer interfaces as the potential applied to the Au(110) electrode is varied.

II. EXPERIMENTAL SECTION

The experiments were conducted on a variant of the CPR protein, P499C, generated by site directed mutagenesis using a truncated form of the wild-type protein that lacks the helical *N*-terminal region that is required to anchor the protein on the endoplasmic reticulum [6]. P499C thus has a cysteine group on the solvent accessible surface of the protein which binds to the Au(110) surface [6]. The potentials of the oxidized and reduced forms of the P499C variant have been determined [6]. The preparation of ordered monolayers of P499C at the Au(110)–phosphate buffer interface has been described in detail previously [5,6] as have the electrochemical cell, the potentiostat, and the RAS instrument [5,6,10,11]. The latter yields a linear optical signal that is the difference in reflectivity from two orthogonal directions in the surface of plane polarized light at normal incidence and reflection from the crystal. For a cubic substrate this geometry results in a cancellation of the bulk signal by symmetry and RAS becomes a probe of surface anisotropy [10]. The measured reflection anisotropy (RA) signal from 1.5 to 5.5 eV is given by

$$\mathrm{Re}\left(\frac{\Delta r}{r}\right) = \mathrm{Re}2\left(\frac{r_{[1\bar{1}0]} - r_{[001]}}{r_{[1\bar{1}0]} + r_{[001]}}\right), \tag{1}$$

where $r_{[1\bar{1}0]}$ and $r_{[001]}$ are the reflection coefficients in the $[1\bar{1}0]$ and [001] directions in the (110) surface, respectively, and $^{r}/_{2}$ is the average of these quantities.

As in the previous work [5,6,9] the solutions used were NaH_2PO_4 and K_2HPO_4 (BDH, Analar grade) prepared with Millipore ultrapure water (18 MΩcm) and made oxygen free by purging with argon prior to use.

In two experiments, five months apart, Au(110)–phosphate buffer interfaces were prepared by flame annealing of a Au(110) crystal [12–14]. In each experiment the RAS profile of the Au(110)–phosphate buffer interface was first recorded for each of the redox potentials of P499C in solution; 0.056, −0.376, −0.465, −0.557, and −0.652 V [6]. In the first experiment P499C was adsorbed at the Au(110)–buffer interface at an applied potential of 0.056 V corresponding to the oxidized state of the protein. The potential was then varied in the sequence −0.376 to −0.652 to 0.056 V and a RAS profile was taken at each potential. The recording of each RAS profile takes ∼7 min. In the second experiment P499C was adsorbed at an applied potential of −0.652 V corresponding to the most reduced state of the protein. The potential was then varied in the sequence −0.557 to 0.056 to −0.652 V and a RAS profile was taken at each potential. Adsorption at both potentials is known to lead to the formation of ordered monolayers in the Au(110) surface [5,6].

*Author to whom correspondence may be addressed: peterw@liverpool.ac.uk

The redox potentials for the different redox states of P499C CPR were measured electrochemically by redox titration. Redox titration was carried out under anaerobic conditions in a Belle Technology glovebox (Belle Technology) under a nitrogen atmosphere (oxygen maintained at <2 ppm). Prior to titration, the protein was fully oxidized using potassium ferricyanide and loaded onto a BioRad Econo-Pac 10DG gel filtration column. The final concentration of CPR used in the titrations was 40 μM. For reductive titration, sodium dithionite was used as reductant and the redox mediators (0.3 μM methyl viologen, 1 μM benzyl viologen, 7 μM 2-hydroxy-1, 4-naphthoquinone, and 2 μM phenazine methosulfate) were added to assist electrical communication. After each addition of reductant, 5 min of equilibration time was allowed to stabilize the electrodes. This process was repeated until the protein was fully reduced as ascertained by generation of five overlapped spectra. Absorption spectra (typically 40–50) were recorded from 1.6 to 4.1 eV. Spectra of the different redox states were generated by global fitting (specfit/32) and redox potentials were calculated by analysis of absorption data at a single wavelength as previously described [15].

III. RESULTS

The RAS profiles of the Au(110)–buffer interface in the first experiment obtained at applied potentials of −0.652 to 0.056 V, the redox potentials of P499C, are shown in Fig. 1. Very similar RAS profiles were obtained for the Au(110)–buffer interface in the second experiment and the difference between the two profiles obtained at applied potentials of −0.652 V are shown by the crosses in Fig. 1. The total anisotropy measured on the Au crystal in the second experiment was 8% higher than that in the first experiment. The actual difference may be lower since this measurement is sensitive to the uncertainty of $\pm 4^{\circ}$ in the determination of the optimum azimuthal angle in the Au(110) plane between the plane of polarization of the incident light and the principle axes of the Au(110) surface [5]. A more significant difference between the two experiments was in the position of the origin of the RAS signal which was 1.2×10^{-3} lower in the second experiment. This is an instrumental effect arising from slight differences of the order of minutes of arc in the alignment of the first polarizer [13]. These differences

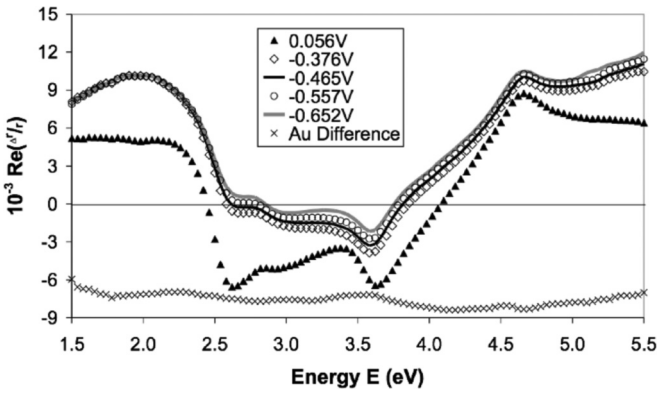

FIG. 1. RA spectra of Au(110) as a function of applied voltage in 0.1 M NaH_2PO_4-K_2HPO_4 at pH 7.2. The difference between the two experiments on Au(110) (×) is shifted down by 7 units on the y axis.

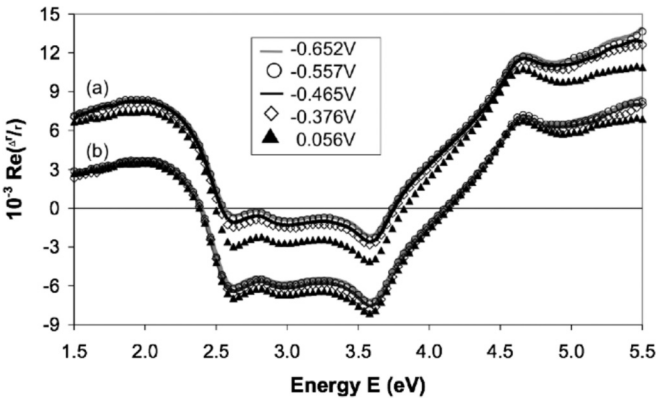

FIG. 2. RA spectra of Au(110) + P499C CPR for (a) forward direction and (b) reverse direction recorded in 0.1 M NaH_2PO_4-K_2HPO_4 at pH 7.2. The scans in part (b) have been shifted down by 4 units on the y axis.

between the two experiments do not have a significant effect on the analysis that follows and were minimized by a scaling of the results obtained for the RAS profiles of the Au(110)–buffer interface in the two experiments.

The RAS profiles of the ordered monolayer of P499C adsorbed on the Au(110)–phosphate buffer interface at −0.652 V and obtained as the potential is taken sequentially through the redox potentials to 0.056 V are shown in Fig. 2(a) and in the reverse sequence 0.056 to −0.652 V in Fig 2(b). The results obtained for the reverse potential sequence have been shifted down by 4 units on the y axis for clarity. The RAS profiles of P499C adsorbed on the Au(110)–phosphate buffer interface at 0.056 V and obtained as the potential is taken sequentially through 0.056 to −0.652 V are shown in Fig 3(a) and in the reverse sequence −0.652 to 0.056 V in Fig 3(b). The results obtained for the reverse potential sequence have been shifted down by 5 units on the y axis for clarity. There are subtle differences in these profiles that are difficult to discern on the scale of Figs. 2 and 3.

The spectra recorded during the redox titration are shown in Fig. 4. Characteristic flavin absorbance maxima at $\varepsilon_{3.26\,eV}$ and $\varepsilon_{2.73\,eV}$ were observed for fully oxidized P449C CPR. As

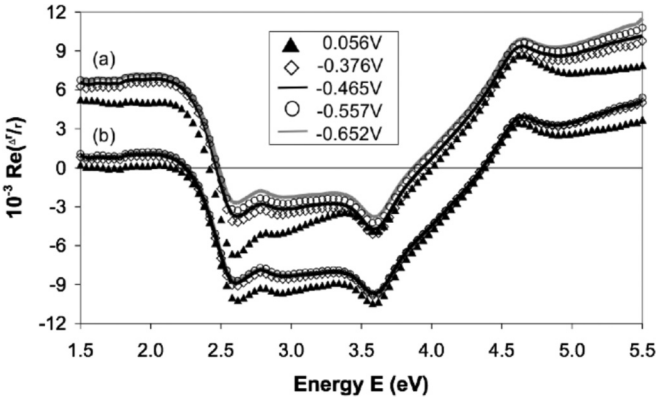

FIG. 3. RA spectra of Au(110) + P499C CPR for (a) forward direction and (b) reverse direction recorded in 0.1 M NaH_2PO_4-K_2HPO_4 at pH 7.2. The scans in part (b) have been shifted down by 5 units on the y axis.

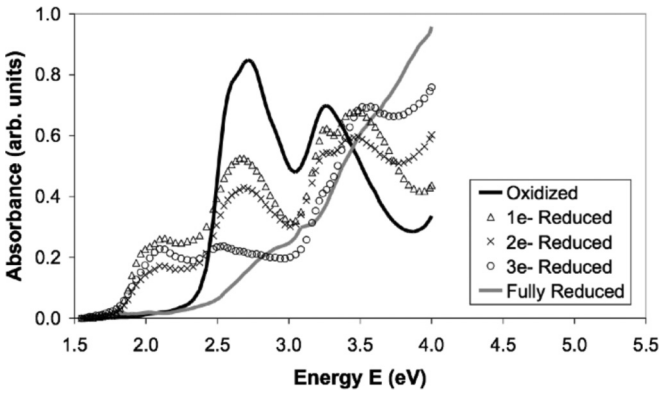

FIG. 4. Ultraviolet-visible spectrum of P499C CPR in 100 mM potassium phosphate, pH 7.2, at 25 °C. The concentration of enzyme was determined spectroscopically using $\varepsilon_{2.73\,eV} = 22\,mM^{-1}\,cm^{-1}$ for oxidized P499C full-length CPR.

reduction proceeded from the oxidized to the semiquinone state (E from approximately −340 to −570 mV), a decrease in absorbance at $\varepsilon_{2.73\,eV}$ and an increase in intensity at $\varepsilon_{2.11\,eV}$ were observed indicating a mixture of partially reduced species of CPR. Further reduction from the predominantly semiquinone to hydroquinone state (E more negative than −570 mV) was indicated by a decrease in the semiquinone signal at $\varepsilon_{2.11\,eV}$ to form the reduced dihydroflavin form of CPR.

IV. DISCUSSION

First, we can eliminate the possibility that the protein denatures on the Au(110) surface since a denatured protein would lose the flavin cofactors and in particular the isoalloxazine rings which make the major contribution to the RAS profiles. A denatured protein would not be redox active and it would not be possible to change the RAS profiles by cycling the potential applied to the electrode.

The RAS profiles of Au(110)–electrolyte interfaces are sensitive to the potential applied to the Au electrode which has a strong influence on the morphology of Au(110) surfaces [10,12–14,16–19]. The RAS profiles of the Au(110)–phosphate buffer interface (Fig. 1) at the four negative potentials are very similar to the RAS profile observed for the (1 × 3) surface reconstruction adopted by the Au(110) surface in a variety of electrolytes in this potential range [13,14]. As the applied potential is made more positive the RAS profiles of Au(110)–electrolyte interfaces in some electrolytes first adopt a profile associated with the (1 × 1) surface structure and eventually one associated with a (1 × 1) anion induced structure resulting from the adsorption of anions [13,14]. The RAS profile observed at 0.056 V is very similar to that observed from an anion induced (1 × 1) Au(110) surface structure [13,14].

A comparison of Figs. 1–3 shows that the adsorption of the protein significantly reduces the sensitivity of the RAS profiles to the applied potential and that there are significant irreversible effects on the RAS profiles of the adsorbed protein when the potential is stepped through 0.056 V (Fig. 2) and −0.652 V (Fig. 3). The most noticeable difference between the RAS profiles of the Au(110)–buffer interface (Fig. 1) and those of the adsorbed protein occurs for the applied potential of 0.056 V. This difference is very likely to be due to the replacement of the weakly adsorbed anions on the Au(110)–buffer interface by the CPR which makes a strong Au-S bond with the Au(110) surface [5,6]. Previous work shows [20–22] that this bond is not disrupted by variations in the applied potential so the anions will not be able to return to the surface as the potential is varied. The main differences between the RAS profiles of the adsorbed proteins and the Au(110)–interface are a reduction in the intensity of the broad positive peak centered on ∼2.0 eV and an increased, negative, intensity in the region of 2.5 to 3.5 eV. The latter has been associated with the formation of the Au-S bond and the contribution of the isoalloxazine rings [6].

When the protein is adsorbed at −0.652 V, corresponding to the protein in its most reduced state, the intensity of the RAS profile becomes progressively more negative as the potential is increased [Fig 2(a)]. However once the potential reaches 0.056 V, corresponding to the oxidized state of the protein, the RAS profiles obtained subsequently at the reducing potentials, while becoming less negative, do not return to the original values [Fig 2(b)]. Similarly when the protein is adsorbed at 0.056 V the RAS profiles obtained at the reducing potentials become less negative [Fig 3(a)] but when the potential reaches −0.652 V the RAS profiles obtained as the potential is increased, while becoming more negative, do not return to the original values and in particular the profile obtained at 0.056 V is significantly different from that obtained after the adsorption [Fig 3(b)]. In summary the weakest and strongest RAS profiles are obtained when the protein is adsorbed at −0.652 and 0.056 V, corresponding to the reduced and oxidized forms, respectively. Taking these profiles as the signatures of the most reduced and most oxidized forms of the protein on the Au(110) surface then once the protein has been reduced it cannot subsequently be fully oxidized and once the protein has been oxidized it cannot subsequently be fully reduced.

Figure 5 is a schematic representation of what is known about the P499C protein adsorbed on the Au(110) surface.

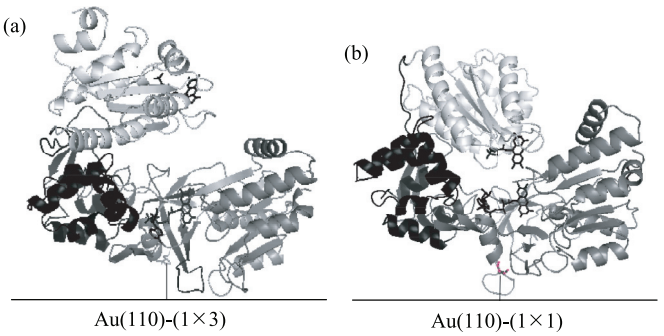

FIG. 5. Schematic showing (a) the reduced and (b) the oxidized form of P499C CPR adsorbed on the Au(110) surface. The FMN-binding domain is shown in light gray, the connecting domain in black, and the FAD/NADP domain in dark gray. The FAD and FMN cofactors are shown as sticks. It is important to note that the molecules are not isolated on the surface but are arranged in an ordered monolayer. The schematic protein structure is derived from that of rat cytochrome P450 reductase [1]. The protein data accession code is 1AMO.

Adsorption at 0.056 and −0.652 V gives rise to ordered monolayers of P499C with each molecule bonded to the Au(110) surface by the formation of a Au-S bond and probably a large number of secondary interactions since a consideration of the size of the protein [1] and the Au(110) surface unit cell indicates the protein occupies the surface area of ∼360 Au atoms. Prior to adsorption the Au(110) surface is expected to be in the open (1×3) structure at −0.652 V and in a closed (1×1) structure occupied by weakly adsorbing anions at 0.056 V [13,14]. In solution the protein is in the "closed" oxidized form at 0.056 V and in the "open" reduced form at −0.652 V with open and closed referring to the relative orientation of the FAD and FMN cofactors each of which supports an optically active isoalloxazine ring [1–3]. The isoalloxazine rings are responsible for the functional activity of the protein and previous work has shown that when the protein is adsorbed on the Au(110) surface at −0.652 and 0.056 V the planes of the isoalloxazine ring structures are orientated roughly vertical to the surface and directed along either the $[1\bar{1}0]$ or [001] direction of the Au(110) surface [5,6].

There are a number of possible origins for the potential induced changes in the RAS profiles shown in Figs. 2 and 3. First, these changes could arise from contributions from the Au(110) substrate (Fig. 1) though this seems unlikely given that the effect of the adsorbed protein is to reduce the dependence of the RAS profile on the applied potential. Second, since it is established that the dominant contribution to the RAS profile of the adsorbed CPR arises from the isoalloxazine rings [6], the planes of which are orientated vertically to the surface, the different RAS profiles could arise from potential induced changes in the orientation of the whole protein on the surface similar to that found for adenine [7,8]. This would probably require changes not just in the Au-S bond but in a number of other interactions between the protein and the Au surface. Finally the difference in RAS profiles could arise from changes in the orientation of the FAD and FMN domains, similar to those that occur in solution [1–3], as a function of redox potential and which are illustrated for the "open" and "closed" forms in Fig. 5. This latter possibility might also explain the irreversible changes noted above given the different structures of the oxidized and reduced forms of the protein. The morphology of the Au(110) substrate clearly determines the order of the adsorbed monolayers of protein [5] and this morphology is very different at the two potentials, being an open $\sim(1 \times 3)$ structure at −0.652 V and probably a more closed $\sim(1 \times 1)$ structure when the adsorbed anions are removed by the adsorbing CPR at 0.056 V. Thus a monolayer of the molecule adsorbed in a closed form on the $\sim(1 \times 1)$ Au(110) surface at 0.056 V may not have the freedom to return to this structure once the protein is reduced and structural changes take place in the configuration of neighboring molecules on the Au(110) substrate. Similar hindrance from interactions between neighboring molecules may limit the freedom of the molecule to respond to changes in the applied potential when the molecule is adsorbed at −0.652 V.

As in previous work [7–9,20–24] we assume that the RAS of the adsorbed molecules is the sum of the contribution from the molecules and from the Au(110) surface together with the contribution from the Au-S bond. Figure 6 shows the difference between the RAS profiles of Figs. 1 and 2(a) at each potential,

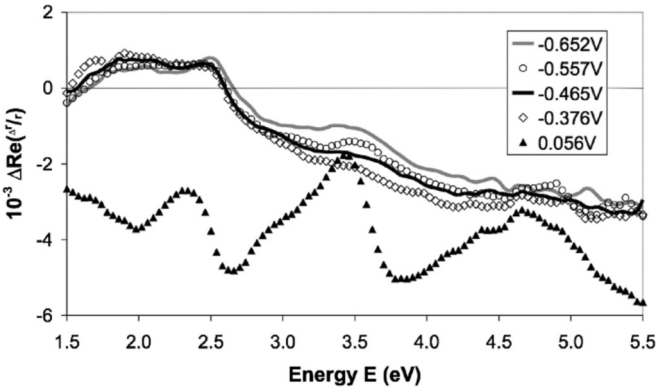

FIG. 6. RA spectra of P499C CPR obtained by subtracting the corresponding Au(110) from the Au(110) + CPR. All the spectra have been multiplied by −1 for ease of comparison with the absorbance spectra in Fig. 4.

which might be attributed to the RAS of the adsorbed species. The large variation in the difference spectra obtained for 0.056 V in Fig. 6 reflects the very different RAS observed from the Au(110) at this potential due to the adsorbing of anions and potential induced reconstructions [13,14]. Once a monolayer of CPR is adsorbed on the surface at −0.652 V it is unlikely that the anions will displace the protein and adsorb on the Au(110) surface when the potential is changed to 0.056 V. Consequently the difference spectrum shown in Fig. 6 will not be a true reflection of the RAS of the adsorbed species at this potential. Figure 7 shows the difference between the RAS profiles of the adsorbed protein on Au(110) at each potential [Figs. 2(a) and 2(b)] and the RAS profile of the Au(110) at −0.652 V, the potential at which the P499C was initially adsorbed. This approach produces spectral differences with almost identical shapes at all potentials but different intensities, the only significant difference in shape occurring above 4.5 eV for the results obtained at 0.056 V. This result suggests that, as found for cytosine [23,24], the adsorption of the protein "freezes" the Au(110) surface structure in the $\sim(1 \times 3)$ structure present at −0.652 V. This "freezing" of the Au(110) surface may not be complete since unlike the cytosine case there are still differences in the intensities of the profiles formed by subtracting the RAS of the Au at the potential at which the molecule was adsorbed. These differences in intensity are considered later.

Since the adsorption of P499C on the Au(110) interface at 0.056 V is expected to displace the anions it is likely that the Au(110) surface will transform to a (1×1) structure [13,14] following the adsorption of the molecule. The RAS profile of this (1×1) structure has not been obtained at this potential in the phosphate buffer. Consequently it is not possible to perform an equivalent comparison of difference spectra for the RAS profiles obtained following adsorption at 0.056 V to that shown in Fig. 7 for the results obtained following adsorption at −0.652 V. However profiles very similar to those shown in Figs. 7(a) and 7(b) are obtained when the RAS profile of the Au(110)–buffer interface is subtracted from the RAS profiles shown in Fig. 3(b), suggesting that following adsorption at 0.056 V a subsequent change in the applied potential to −0.652 V causes the Au surface to adopt a "frozen"

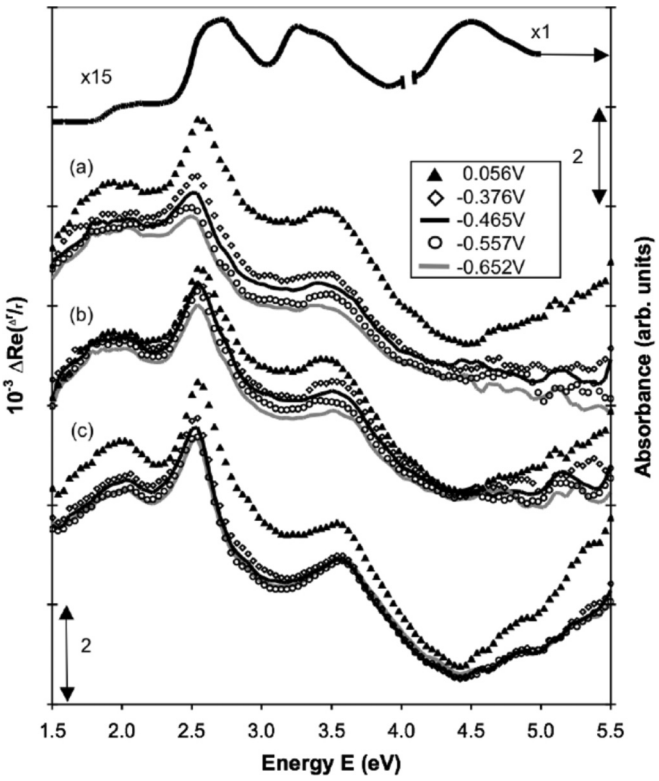

FIG. 7. The top curve shows the uv-visible spectrum of P499C CPR as reported earlier [6]. The spectral region 1.5 to 4.0 eV has been increased in intensity by a factor of 15. The spectral profiles (a)–(c) are the differences between the RAS profile of the Au(110) surface at −0.652 V and the RAS profiles shown in Figs. 2(a), 2(b), and 3(c) all multiplied by −1 for comparison with the top curve and the uv-visible spectrum in Fig. 4.

configuration even when covered by a monolayer of the protein. These profiles are shown in Fig. 7(c). In terms of the expected redox state of the protein on the surface the curves in each sequence, (a)–(c) in Fig. 7, the most intense corresponds to the oxidized form and the intensities decrease as the protein is reduced by one, two, three, and four electrons, respectively.

The full curve at the top of Fig. 7 is the uv-visible absorbance spectrum of 8.3 μM of P499C in the phosphate buffer solution reported earlier [6]. In the light of the results of Fig. 4 the P499C was probably in an incompletely oxidized form in the earlier experiments. This spectrum shows three features which can be clearly recognized in the profiles of Figs. 7(a)–7(c): a low energy broad feature between 2.0 and 2.3 eV; a broad feature between 2.5 and 3.0 eV, which in the gas phase peaks at 2.7 eV; and to higher energy a broad peak between 3.0 and 3.8 eV. There is also a very strong peak centered on 4.5 eV in the absorbance spectrum of the protein in solution. The features at 2.7 eV and 3.0 to 3.8 eV and a stronger peak at 4.3 to 4.7 eV are associated with the contributions from the isoalloxazine rings [25–28].

A comparison of the absorption spectrum of the protein in solution (Fig. 4) with the RAS profiles of Fig. 7 provides insight into the redox states of the adsorbed protein at different applied potentials. The intensity of the low energy feature between 2.0 and 2.3 eV, which is not associated with the isoalloxazine rings, is very sensitive to the redox state of the protein (Fig. 4). The intensity of this feature in the RAS profiles indicates that the adsorbed protein is not completely oxidized even at 0.056 V. This view is supported by the position of the feature, associated with the isoalloxazine rings, peaking at 3.5 eV in the RAS profile which at 0.056 V is closer to that of a slightly reduced form of the protein in solution (Fig. 4). The energy of this feature in the absorbance spectrum of the isoalloxazine rings in solution is also sensitive to the solution and can vary in position by ∼0.4 eV [26]. The adsorbed protein is also not fully reduced at −0.652 V since in the absorbance spectrum of the reduced form in solution all the prominent features in the spectrum disappear and are replaced by a smoothly rising contribution from ∼2.0 eV onwards (Fig. 4).

When the protein is adsorbed on the Au(110) surface the peak centered on 2.7 eV in solution overlaps with the contribution from the Au-S bond at 2.5 eV. Even though the separation of these two peaks is too small for them to be resolved they are distinct since their intensities have a different time dependence during the adsorption process [6]. After allowing for the contribution from the Au-S bond the relative intensity of the three low energy features in the incompletely oxidized form of the protein in solution is comparable to their relative intensity in the spectra from the oxidized form of the adsorbed protein (Fig. 7). The intense peak centered on 4.5 eV in the spectrum observed in solution arises from a number of contributions. These include a strong peak from the isoalloxazine rings, the intensity of which is very sensitive to the environment [26], and the large number of aromatic amino acids in the protein, phenylalanine, tyrosine, and tryptophan. The aromatic amino acids are distributed throughout the structure of the protein and there is no significant order in the directions of their optical dipoles so it is unlikely that there will be significant net anisotropy in their contribution to the RAS profile even when the protein forms an ordered monolayer on the Au(110) surface [6]. This explains the absence of a strong contribution from the aromatic amino acids in the high energy region of the spectrum of the adsorbed protein. The origin of the broad feature in the RAS profiles that increases in intensity from 4.5 eV is unknown. It could be associated with the high energy feature observed in the absorbance spectrum of the isoalloxazine rings in solution [25–28].

Useful insight into the behavior of the protein on the Au(110) surface can be obtained by comparing the profiles of Fig. 7 with those of the protein in solution at different redox potentials (Fig. 4). Ignoring the possibility of subtle effects in the relative intensity of spectral contributions to the RAS profiles arising from potential induced changes in the orientation of the protein, or of components of the protein, on the Au(110) surface the dependence of the intensities of the two features in the middle of the spectrum, arising from the isoalloxazine rings, is broadly consistent with the behavior observed in solution. This comparison is complicated by the presence of the Au-S peak at 2.5 eV which overlaps with the low energy contribution from the isoalloxazine rings which peaks at 2.7 eV. In solution the 2.7 eV feature is the most intense in the oxidized form, in agreement with what is observed from the protein on the Au(110) surface. As the protein is reduced in solution both peaks in the spectrum of the isoalloxazine rings lose intensity, with the low energy

peak losing intensity more rapidly (Fig. 4). Although the adsorbed protein does not become completely reduced this trend is also observed in the RAS profiles of the protein on the Au(110) surface particularly when the potential dependence of the RAS peak arising from the Au-S bond is taken into account. Previous studies of the RAS of the Au-S bond formed on Au(110) at −0.6 V by cysteine, cystine [20], a cysteine-tryptophan dipeptide [21], and decanethiol [22] show that it contributes a symmetric peak located at 2.5 eV with a width of ∼0.3 eV at full width at half maximum. In the RAS of these smaller molecules [20,21] adsorbed on Au(110) this feature remains sharp but reduces in intensity by 50% when the applied potential is increased to 0.0 V. This intensity variation is opposite to the behavior shown in Fig. 7 so as the potential is made more negative the increase in intensity of the Au-S peak at 2.5 eV is expected to mask, to some extent, the fall in intensity of the 2.7 eV contribution from the isoalloxazine rings. That this does happen is confirmed by a narrowing of this feature in the RAS profile to a more symmetric profile, caused by a reduction in intensity on the high energy side and a shift to lower energy of ∼0.2 eV in the position of the maximum intensity as the potential is reduced from 0.056 V. In summary Fig. 7 provides strong support for the assumption that the RAS profile of the adsorbed protein is the sum of contributions from the Au(110) and the protein and the hypothesis that the adsorption of the protein at −0.652 V "freezes" the Au(110) surface in a ∼(1 × 3) structure. It also confirms the previous finding [6] that the RAS profile of CPR on the Au(110)–buffer interface arises primarily from the isoalloxazine rings.

While the spectral profiles shown in Figs. 7(a)–7(c) have very similar shapes they have different absolute intensities and differences in the relative intensity of spectral features. These differences in intensity arise not only from variations in the applied potential but also in the sequence in which the applied potentials are varied, as is also clear from Figs. 2 and 3. The differences in the relative intensity of spectral features observed at the *same* value of the applied potential is particularly instructive since the contribution to the RAS profile from the Au(110) surface should certainly cancel and any differences in the contribution of the protein should reflect differences in the history of redox potential changes. Given the irreversible changes observed in the RAS profiles as the applied potential is varied, the fact that the protein adopts ordered monolayer structures when adsorbed on the Au(110) surface in both the oxidized and reduced states and that in solution the protein adopts very different conformations in the oxidized and reduced states, it is reasonable to suppose that the differences observed are the result of potential induced conformational changes in the adsorbed protein. Additional support for this hypothesis comes from the observation that the main contributions to the RAS profiles of the adsorbed protein arise from dipole transitions aligned in the planes of the isoalloxazine rings, that these planes are orientated vertical to the surface [5,6], and that variations of the redox potential in solution change the alignment of the planes of the two rings [1–3]. These arguments together with the observations that the dipole transitions are primarily in plane and polarized along the long axis of the isoalloxazine rings [25,27] and that these directions are essentially independent of the oxidation state

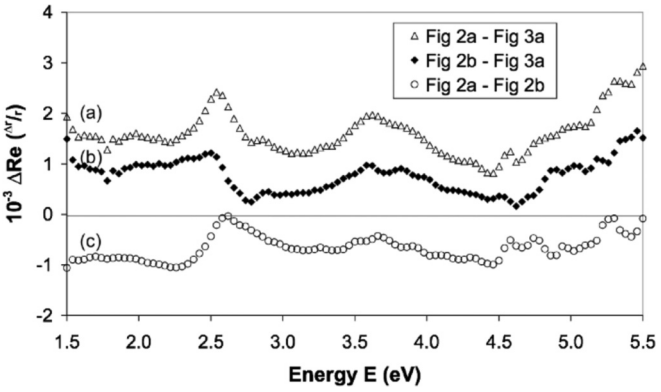

FIG. 8. The differences in the RAS profiles obtained at −0.652 V. The differences between the profiles of Figs. 2 and 3 are corrected for the differences in the RAS of the Au(110) surface obtained at −0.652 V (Fig. 1) in the two experiments.

of the molecules [27] open up the possibility of monitoring conformational change in the adsorbed proteins by varying the applied potential.

Figures 2 and 3 show that as noted earlier there are subtle differences between the three RAS profiles of the adsorbed protein obtained at −0.652 V (Figs. 2 and 3) that arise from differences in the potential at which the protein was adsorbed on the Au(110) surface and the sequence in which the potentials were varied. There are similar differences between the three RAS profiles of the adsorbed protein obtained at 0.056 V.

The differences in the RAS profiles obtained at −0.652 V are shown in Fig. 8: the top profile (a) is the difference between Figs. 2(a) and 3(a), profile (b) is the difference between the Figs. 2(b) and 3(a), and profile (c) is the difference between Figs. 2(a) and 2(b).

The profiles shown in Fig. 8 reveal five spectral components, the intensities of which depend on the history of the variation in the applied potential. In order of increasing energy these are a broad low energy feature below 2.3 eV that is very weak in all the profiles; a narrow peak at 2.5 eV associated with the Au-S bond; two broad features associated with the isoalloxazine rings, one to high energy of the Au-S bond and one in the range of 3.5 to 4.0 eV; and a high energy feature beyond 4.5 eV of unknown origin but possibly associated with the isoalloxazine rings. It is important to note that the differences shown in Fig. 8 are between RAS profiles measured at the same applied potential so the protein should be in the same redox state and contributions from the Au(110) should cancel. In these circumstances the only contributions to the spectral profiles of Fig. 8 should arise from changes in the order or orientation of transition dipoles on the Au(110) surface arising from irreversible structural changes arising from the history of the applied potentials.

The Au-S bond is known to give rise to a symmetrical peak at 2.5 eV. This peak is clearly seen in Fig. 8(a). Its presence in this and the other spectra of Fig. 8 indicates that the Au-S bond may change its order or orientation on the surface as a result of changes in the sequence of applied potentials. The Au-S peak is overlapped by contributions on the low energy side in Fig. 8(b) and on the high energy side in Fig. 8(c). In solution the low

energy feature, which is not associated with the isoalloxazine rings, has a negligible intensity in the fully reduced state of the protein (Fig. 4). However although all the spectra shown in Figs. 8(a)–8(c) are differences between RAS profiles taken at −0.652 V, it has been established that the protein is not completely reduced on the Au(110) surface at this potential. Consequently the variation in the intensity of the low energy feature in Fig. 8 is consistent with changes in the order or orientation of incompletely reduced proteins on the Au(110) surface. The incomplete reduction of the protein at −0.652 V on the Au(110) surface explains the presence of the features, one peaking at 2.7 eV and the other in the range of 3.4 to 4.0 eV, associated with the isoalloxazine rings. These features change in both absolute and relative intensity in the profiles shown in Fig. 8. The 2.7 eV feature is almost absent in Figs. 8(a) and 8(b) but is quite strong in Fig. 8(c), inducing a shift in the energy of the combined Au-S bond and isoalloxazine ring contribution to 2.6 eV. In contrast the intensity of the feature peaking at 3.5 eV in Fig. 8 and associated with the isoalloxazine rings is strongest in Fig. 8(a), weaker in Fig. 8(b), and weakest in Fig. 8(c). These two contributions from the isoalloxazine rings are known to arise from dipole transitions polarized in the planes of the rings and in directions close to the long axis of the rings [25–28]. Different studies give angles for the 2.7 eV transition of 0°, 15°, and 32° [25–27] with respect to the long axis with corresponding values of 11°, 10°, and 10° [25–27] for the 3.5 eV transition. It is important to note that all the studies [25–27] agree that there is a significant angle between the directions of the two transitions and consequently, as illustrated in several other cases [7,8,23,24], this makes it possible to deduce from the angular variation of the RAS results [5,6] that the plane of the isoalloxazine rings is orientated roughly vertical to the Au(110) surface. Any changes in the orientation of the rings in this plane will result in variations in the absolute and relative intensity of these contributions to the RAS profiles. A reasonable explanation of the changes in both the absolute and relative intensity of these two features in the profiles shown in Fig. 8 is that variations in the applied potential gave rise to irreversible changes in the relative orientation of the two isoalloxazine rings on the Au(110) surface. If this explanation is correct then it should be possible to use RAS to monitor these conformational changes in real time as the potential applied to the Au(110) electrode is varied. This will not be possible using the standard RAS instrument employed in this work because the spectra are recorded sequentially and the experiment is rather slow. However this may be possible with the rapid RAS instrument [6,29] which records a number of wavelengths simultaneously on a faster timescale. This will make it possible to explore whether the potential induced changes in the RAS profiles all occur on the same timescale. Such studies are in progress.

V. CONCLUSIONS

Components of the absorption spectrum of cytochrome P450 reductase, including two features associated with the isoalloxazine rings, have been identified in the RAS profiles of ordered monolayers of the protein adsorbed at Au(110)–buffer interfaces. The dependence of the intensity of these spectral features on the applied potential is consistent with spectral changes expected as the redox potential of the protein is varied, although the protein does not become fully reduced or fully oxidized on the Au(110) surface. Variations in the applied potential give rise to irreversible changes in the RAS profiles which can be associated with conformational changes of the protein on the Au(110) surface. Future experiments with a rapid RAS instrument may make it possible to determine whether these conformational changes take place on the same timescale.

ACKNOWLEDGMENTS

The authors acknowledge financial support from the UK Biotechnology and Biological Science Research Council (BBSRC, Grant No. BB/F004400/1). J.H.C. is supported by a Ph.D. award funded by the UK Engineering and Physical Science Research Council (EPSRC). N.S.S. acknowledges support from an EPSRC Established Career Fellowship and a Royal Society Wolfson Merit Award.

[1] M. Wang, D. L. Roberts, R. Paschke, T. M. Shea, B. S. Masters, and J. J. Kim, Proc. Natl. Acad. Sci. USA **94**, 8411 (1997).

[2] S. Hay, S. Brenner, B. Khara, A. M. Quinn, S. E. J. Rigby, and N. S. Scrutton, J. Am. Chem. Soc. **132**, 9738 (2010).

[3] C. R. Pudney, B. Khara, L. O. Johannissen, and N. S. Scrutton, PLoS Biol. **9**, e1001222 (2011).

[4] S. Brenner, S. Hay, A. W. Munro, and N. S. Scrutton, FEBS J. **275**, 4540 (2008).

[5] C. I. Smith, J. H. Convery, B. Khara, N. S. Scrutton, and P. Weightman (unpublished).

[6] J. H. Convery, C. I. Smith, B. Khara, N. S. Scrutton, P. Harrison, T. Farrell, D. S. Martin, and P. Weightman, Phys. Rev. E **86**, 011903 (2012).

[7] C. I. Smith, A. Bowfield, G. J. Dolan, M. C. Cuquerella, C. P. Mansley, D. G. Fernig, C. Edwards, and P. Weightman, J. Chem. Phys. **130**, 44702 (2009).

[8] A. Bowfield, C. I. Smith, G. J. Dolan, M. C. Cuquerella, C. P. Mansley, and P. Weightman, e-J. Surf. Sci. Nanotechnol. **7**, 225 (2009).

[9] H. L. Messiha, C. I. Smith, N. S. Scrutton, and P. Weightman, Europhys. Lett. **83**, 18004 (2008).

[10] P. Weightman, D. S. Martin, R. J. Cole, and T. Farrell, Rep. Prog. Phys. **68**, 1251 (2005).

[11] D. E. Aspnes, J. P. Harbison, A. A. Studna, and L. T. Florez, J. Vac. Sci. Technol., A **6**, 1327 (1988).

[12] O. M. Magnusson, J. Wiechers, and R. J. Behm, Surf. Sci. **289**, 139 (1993).

[13] C. I. Smith, A. Bowfield, N. J. Almond, C. P. Mansley, J. H. Convery, and P. Weightman, J. Phys.: Condens. Matter **22**, 392001 (2010).

[14] C. I. Smith, P. Harrison, T. Farrell, and P. Weightman, J. Phys.: Condens. Matter **24**, 482002 (2012).

[15] A. W. Munro, M. A. Noble, L. Robledo, S. N. Daff, and S. K. Chapman, Biochemistry **40**, 1956 (2001).

[16] B. Sheridan, D. S. Martin, J. R. Power, S. D. Barrett, C. I. Smith, C. A. Lucas, R. J. Nichols, and P. Weightman, Phys. Rev. Lett. **85**, 4618 (2000).
[17] V. Mazine, Y. Borensztein, L. Cagon, and P. Allongue, Phys. Status Solidi A **175**, 311 (1999).
[18] V. Mazine and Y. Borensztein, Phys. Rev. Lett. **88**, 147403 (2002).
[19] P. Weightman, C. I. Smith, D. S. Martin, C. A. Lucas, R. J. Nichols, and S. D. Barrett, Phys. Rev. Lett. **92**, 199707 (2004).
[20] R. LeParc, C. I. Smith, M. C. Cuquerella, R. L. Williams, D. G. Fernig, C. Edwards, D. S. Martin, and P. Weightman, Langmuir **22**, 3413 (2006).
[21] B. M. della Rocca, C. I. Smith, C. Tesauro, A. Desideri, and P. Weightman, Surf. Sci. **604**, 2170 (2010).
[22] A. Bowfield, C. I. Smith, M. C. Cuquerrella, T. Farrell, D. G. Fernig, C. Edwards, and P. Weightman, Phys. Status Solidi C **5**, 2600 (2008).
[23] P. Weightman, G. J. Dolan, C. I. Smith, M. C. Cuquerella, N. J. Almond, T. Farrell, D. G. Fernig, C. Edwards, and D. S. Martin, Phys. Rev. Lett. **96**, 086102 (2006).
[24] C. P. Mansley, C. I. Smith, A. Bowfield, D. G. Fernig, C. Edwards, and P. Weightman, J. Chem. Phys. **132**, 214708 (2010).
[25] T. Climent, R. González-Luque, M. Merchán, and L. Serrano-Andrés, J. Phys. Chem. A **110**, 13584 (2006).
[26] L. B.-Å. Johansson, Å. Davidsson, G. Lindblom, and K. R. Naqvi, Biochemistry **18**, 4249 (1979).
[27] M. Salim, U. Siddiqui, G. Kodali, and R. J. Stanley, J. Phys. Chem. B **112**, 119 (2008).
[28] M. Sun, T. A. Moore, and P. S. Song, J. Am. Chem. Soc. **94**, 1730 (1972).
[29] P. Harrison, T. Farrell, A. Maunder, C. I. Smith, and P. Weightman, Meas. Sci. Technol. **12**, 2185 (2001).